Journal of Automation and Intelligence 4 (2025) 98–107

Contents lists available at ScienceDirect

Journal of Automation and Intelligence

Research article

Time-synchronized control with the least upper bound of fixed settling time☆

Wanyue Jiang [a], Shuzhi Sam Ge [b], Ruihang Ji [b], Dongyu Li [c,*]

[a] The Institute for Future & Shandong Key Laboratory of Industrial Control Technology, School of Automation, Qingdao University, Qingdao, 266071, China
[b] Department of Electrical and Computer Engineering, National University of Singapore, Singapore, 117576, Singapore
[c] School of Cyber Science and Technology, Beihang University, Beijing, 100191, China

ARTICLE INFO

Keywords:
Time-synchronized convergence
Fixed-time control
Settling-time estimation

ABSTRACT

This paper introduces time-synchronized convergence in fixed-time control, where all system states converge to the origin at the same time before a fixed time instant. Sufficient Lyapunov conditions are derived for fixed-time synchronized control (FTSC). An enhanced estimation method for synchronized settling time (ST) is proposed, with an explicit formula for its least upper bound (LUB), which reduces overestimation compared to existing methods. A switching-based technique is incorporated into the controller to avoid singularities while maintaining compatibility with the time-synchronized design. Simulation results validate the fixed-time synchronization properties and the improved ST estimation, demonstrating smoother output trajectories and reduced energy consumption.

1. Introduction

The temporal requirement is an important performance indicator for control technology. Finite-time control is presented in the literature, where system states are demanded to converge in a finite time [1,2]. The settling time (ST) of a finite-time control system naturally increases with the initial state. However, in many applications [3,4], the convergence of the system is strictly required within some fixed time period. As a higher demand is proposed for the control system, fixed-time control is invented, whose ST is irrelevant to the initial system state [5]. With the proper calculation of the ST, engineers are able to stabilize the system within any expected set-point time value through correspondingly designed control system parameters. The application of fixed-time control includes spacecraft rendezvous and docking operations [6], stabilization control of quantum systems [7], observer-based control of robot manipulators [8], event-triggered control of nonlinear systems [9], etc. Predefined/prescribed-time control, which is presented in recent works [10,11] and considered as a special extension of fixed-time control where the ST is predefined/prescribed and the controller is constructed based on the given time.

Despite the fixed-time convergence, for some applications, system states are expected to reach their target values simultaneously. Considering a robotic hand, its fingertips are required to reach the target position and touch the target object simultaneously in the task of grasping slippery objects. In formation assembling tasks, fixed-wing vehicles should reach the desired formation state time-synchronously, otherwise, the very limited output space of the nonholonomic vehicle may lead to the failure of the assembling. Time synchronization of convergence is required for this kind of task. Moreover, time synchronization of convergence brings significant merits to the whole operation [12], e.g., in multi-robot transport, multi-missile cooperative attack, and multi-satellite collaborative observation [6]. In the authors' recent approach [13,14], considering a single-integrator system, a distinctive finite-time controller is proposed for *time-synchronized stability*. However, it is designed for relatively simple system dynamics with accurate mathematical models, and deeper explorations of the fixed-time control case are not provided.

In Fixed-time control, settling time is one of the most important performance specifications. Accurate settling time is difficult to achieve due to various influences, such as nonlinear and un-certain system dynamics, ever-changing convergence rate, external disturbances, etc. Estimation methods are developed to find the least upper bound (LUB) of the ST. The method in [5] is used in the literature [3,15], whereas the bound calculated is found to be much overestimated. An integration-based enhanced ST estimation method is presented in [16] to reduce the overestimation problem, however, it is designed only for the scalar state. The fixed-time-synchronized control (FTSC) differs from common fixed-time control on ST calculation.

Affine systems are widely used as the mathematical model of practical systems [17,18] and Lyapunov conditions have been presented for affine systems to obtain fixed-time convergence [5]. In affine systems, the nonlinear mapping from control input to system output can be well-illustrated by affine equations. When the state is multi-dimensional, the control system should also be extended to the multi-variable case. Lots of good works have been proposed for such a purpose, the control input defined on the error vector [19], the multi-dimensional sliding surface where each dimension works for different state component [20], the sign function that couples every state dimension [21], to name a few. However, it is much more non-trivial when fixed-time-synchronized convergence (FTSC) is required for a system, in which the controller should be elegant enough to cooperate with different dimensions of the system and force all state elements to the origin simultaneously within a fixed time. Moreover, disturbances and uncertainties in the system further increase the difficulty of the controller design.

Motivated by the above, we aim to address the control problem of multi-variable systems under external disturbances, where all the state elements converge *time-synchronously in a fixed time*, i.e., at the same ST whose bound is independent of the initial state. The contributions are as follows.

First, this paper addresses the FSTC problem and presents some sufficient Lyapunov conditions to achieve fixed-time-synchronized stability. Such stability not only facilitates the time synchronization and ratio persistence properties of the system state, but also forces the target system to yield the shortest output trajectory, i.e., optimal in terms of the travel length. A second-order affine system with unknown disturbances is adopted as an example for the controller design, where a disturbance observer, a sliding manifold, and a switching control law are presented.

Second, this paper provides an *enhanced settling time estimation* for the FTSC of a system. The existing estimation method cannot be directly used for the fixed-time-synchronized control due to the special design of the norm-normalized sign function. The proposed synchronized settling time estimation is much less conservative compared with the existing upper bound estimation methods, which is verified by comparative analysis.

Last but important, based on the investigation in the present paper, the time-synchronization phenomenon can also be expected in some finite/fixed-time MIMO system control results with proper modifications, whose estimation of the LUB can be more accurate.

In the rest of the paper, we introduce some technical preliminaries (Section 2), present the main results for the least upper bound calculation (Section 3.1), the fixed-time disturbance observer (Section 3.2), the control design and analysis (Section 3.3) of fixed-time-synchronized convergence. Simulations and comparative studies are conducted in Section 4, where the merit of the proposed approach is demonstrated. In Section 5, pertinent conclusions are finally drawn.

2. Technical preliminaries

We first recall the abbreviations in Table 1 for better clarity.

Table 1
Abbreviations.

FTSC	Fixed-time-synchronized convergence/control
FTSS	Fixed-time-synchronized stable
LUB	Least upper bound
ST	Settling time
RP	Ratio persistent

Consider the affine system

$$\dot{\boldsymbol{x}} = f(\boldsymbol{x}), \tag{1}$$

where $\boldsymbol{x} = \left[x_1, \ldots, x_n\right]^{\mathrm{T}} \in \mathbb{R}^n$ denotes the system state, and function $f : D_0 \to \mathbb{R}^n$ is continuous with $f(0) = 0$. $D_0 \subseteq \mathbb{R}^n$ is an open set with the origin inside. The solution of the system (1) is assumed to be unique for all initial conditions. Let $\boldsymbol{x}(t_0) = \boldsymbol{x}_0$ initially.

Next, we introduce the definitions and tools.

Lemma 1 ([16]). *Given constant parameters $\alpha, \beta, p, g, \chi > 0$ with $p\chi < 1$ and $g\chi > 1$, the following equation holds*

$$\int_0^{+\infty} \frac{\mathrm{d}x}{(\alpha x^p + \beta x^g)^{\chi}} = \frac{B\left(\omega_p, \omega_g\right)}{\alpha^{\chi-\omega_p}\beta^{\omega_p}(g-p)},$$

where $\omega_p = \frac{1-\chi p}{g-p}$, $\omega_g = \frac{\chi g-1}{g-p}$, and the beta function $B(\cdot)$ can be referred to in [22].

Definition 1 ([13]). System (1) is fixed-time-synchronized stable (FTSS) if (1) it is fixed-time stable, i.e., the bounded ST $T(\boldsymbol{x}_0) < T_m < \infty$; (2) the state elements converge time-synchronously, i.e., $x_i(t) \neq 0$ and $\lim_{t \to T(\boldsymbol{x}_0)} x_i(t) = 0$ for $t < T\left(\boldsymbol{x}_0\right)$; and $x_i(t) = 0$ for $t \geq T(\boldsymbol{x}_0)$; where $T\left(\boldsymbol{x}_0\right)$ is the *synchronized settling time* and $T_m > 0$ is a constant. If the above properties hold for any initial states, the system is *globally time-synchronized stable*.

Definition 2 ([13]). The state $\boldsymbol{x}$ is said to be *ratio persistent (RP)*, if for any state elements $x_i(t), x_j(t) \neq 0$, and $i \neq j$, we have $x_i(t)/x_j(t) = c_{ij}$, where c_{ij} is a non-zero constant.

Lemma 2 ([13]). *The state $\boldsymbol{x}$ of system (1) is RP if for $\boldsymbol{x} \neq 0$ and $\zeta \in \{1, -1\}$,*

$$\frac{\boldsymbol{x}}{\|\boldsymbol{x}\|} = \zeta \frac{f(\boldsymbol{x})}{\|f(\boldsymbol{x})\|}.$$

The classical sign function widely used in the literature is written with the subscript 'c',

$$\mathrm{sign}_{\mathrm{c}}\left(x_i\right) = \begin{cases} +1, & x_i > 0, \\ 0, & x_i = 0, \\ -1, & x_i < 0, \end{cases} \tag{2}$$

$$\mathrm{sign}_{\mathrm{c}}(\boldsymbol{x}) = \left[\mathrm{sign}_{\mathrm{c}}\left(x_1\right), \ldots, \mathrm{sign}_{\mathrm{c}}\left(x_n\right)\right]^{\mathrm{T}}, \tag{3}$$

$$\mathrm{sig}_{\mathrm{c}}^{\alpha}(\boldsymbol{x}) = \left[\mathrm{sign}_{\mathrm{c}}\left(x_1\right)\left|x_1\right|^{\alpha}, \ldots, \mathrm{sign}_{\mathrm{c}}\left(x_n\right)\left|x_n\right|^{\alpha}\right]^{\mathrm{T}}. \tag{4}$$

In this paper, the above formulations are normalized and written with subscript 'n'.

Definition 3 ([13]). The *norm-normalized sign function* and its exponential form of vector $\boldsymbol{x}$ are defined as

$$\mathrm{sign}_{\mathrm{n}}(\boldsymbol{x}) \triangleq \begin{cases} \frac{\boldsymbol{x}}{\|\boldsymbol{x}\|}, & \boldsymbol{x} \neq 0, \\ 0, & x = 0, \end{cases} \tag{5}$$

$$\mathrm{sig}_{\mathrm{n}}^{\alpha}(\boldsymbol{x}) \triangleq \|\boldsymbol{x}\|^{\alpha}\mathrm{sign}_{\mathrm{n}}(\boldsymbol{x}). \tag{6}$$

A second-order system is considered for the design of a fixed-time-synchronized controller,

$$\begin{aligned} \dot{\boldsymbol{x}}_1 &= \boldsymbol{x}_2, \\ \dot{\boldsymbol{x}}_2 &= \boldsymbol{f}_0\left(\boldsymbol{x}_1, \boldsymbol{x}_2\right) + \boldsymbol{G}_0\left(\boldsymbol{x}_1, \boldsymbol{x}_2\right)\boldsymbol{u} + \boldsymbol{\Delta}, \end{aligned} \tag{7}$$

where $\boldsymbol{x}_1$ and $\boldsymbol{x}_2$ are system states with n dimensions. For a motion system, $\boldsymbol{x}_1$ can be regarded as a general position vector and $\boldsymbol{x}_2$ can be taken as a velocity vector. The functions $\boldsymbol{f}_0(\boldsymbol{x})$ and $\boldsymbol{G}_0(\boldsymbol{x}) \neq 0$ are known portions, and $\boldsymbol{\Delta}$ denotes the n-dimensional disturbance/uncertainty in the system.

The control objective is to achieve fixed-time-synchronized convergence of System (7) under external disturbance, and present the settling time estimation for the system.

Assumption 1. The initial value, $\boldsymbol{\Delta}(0)$ is bounded within the known constant σ, namely $\|\boldsymbol{\Delta}(0)\| \leq \sigma$. The derivative, $\dot{\boldsymbol{\Delta}}$ is bounded within the known constant δ, namely $\|\dot{\boldsymbol{\Delta}}\| \leq \delta$.

Remark 1. The assumption above is mild in terms of disturbances and commonly used in the literature, e.g., in [19,23]. With bounded $\Delta(0)$ and $\dot{\Delta}$, $\Delta(t)$ is bounded in finite time.

3. Main results

3.1. Settling time for fixed-time-synchronized stability

Inspired by [5], the following definition is presented for the synchronized ST.

Definition 4. If system (1) is FTSS, parameters $\alpha, \beta, p, g, \chi$ are positive, $p\chi < 1$, $g\chi > 1$, the LUB of its synchronized ST satisfies

$$T_{\text{least}} = \sup_{\boldsymbol{x}_0 \in \mathbb{R}^n} \int_0^{V(\boldsymbol{x}_0)} \mathrm{d}V(\boldsymbol{x}) / (\alpha V^p(\boldsymbol{x}) + \beta V^g(\boldsymbol{x}))^{\chi}. \tag{8}$$

Remark 2. In [5], a system is defined as fixed-time stable if its Lyapunov derivative satisfies $\dot{V}(\boldsymbol{x}) \le -(\alpha V^p(\boldsymbol{x}) + \beta V^g(\boldsymbol{x}))^{\chi}$. Integrating both sides of this formula, an upper bound $T(\boldsymbol{x}_0)$ can be calculated under the initial state x_0. The above definition can be used for any finite/fixed-time system that satisfies the Lyapunov condition, whereas it is more appropriate to be defined for a time-synchronized system since every state dimension shares the same ST.

With Definition 4, the following theorem is proposed to guide the controller design and the ST estimation.

Theorem 1. *A system with state x achieves the FTSC, and the ST has the following LUB*

$$T_{\text{least}} = \gamma(\alpha, \beta, p, g, \chi), \tag{9}$$

if the two conditions are satisfied:

i. A Lyapunov function $V(\boldsymbol{x})$ can be found with the first-order derivative

$$\dot{V}(\boldsymbol{x}) \le -(\alpha V^p(\boldsymbol{x}) + \beta V^g(\boldsymbol{x}))^{\chi}, \tag{10}$$

where $\alpha, \beta, p, g, \chi > 0$, $p\chi < 1$ and $g\chi > 1$.

ii. The state $\boldsymbol{x}$ is RP.

Moreover, if the above two conditions hold with $\|\boldsymbol{x}_0\| \to +\infty$, the synchronized ST has an accurate value

$$T(\boldsymbol{x}_0) = T_{\text{least}}.$$

Proof. First, system (1) will be proved as fixed-time stable, namely for $\forall \boldsymbol{x}_0$, $\boldsymbol{x}(t) = 0$ for $t > T(\boldsymbol{x}_0)$. From the condition of fixed-time stability in [5] and noticing (10), we have

$$\begin{aligned} -\mathrm{d}V(\boldsymbol{x}) / (\alpha V^p(\boldsymbol{x}) + \beta V^g(\boldsymbol{x}))^{\chi} &\ge \mathrm{d}t, \\ \int_0^{V(\boldsymbol{x}_0)} \mathrm{d}V(\boldsymbol{x}) / (\alpha V^p(\boldsymbol{x}) + \beta V^g(\boldsymbol{x}))^{\chi} &\ge \int_0^{T(\boldsymbol{x}_0)} \mathrm{d}t \\ &= T(\boldsymbol{x}_0). \end{aligned} \tag{11}$$

Since $V(\boldsymbol{x}_0)$ is monotonically increasing with $\|\boldsymbol{x}_0\|$, $T(\boldsymbol{x}_0) = T_{\text{least}}$ is the LUB when $\|\boldsymbol{x}_0\| \to +\infty$. From Lemma 1, it follows that

$$\begin{aligned} &\sup_{\boldsymbol{x}_0 \in \mathbb{R}^n} \int_0^{V(\boldsymbol{x}_0)} \mathrm{d}V(\boldsymbol{x}) / (\alpha V^p(\boldsymbol{x}) + \beta V^g(\boldsymbol{x}))^{\chi} \\ &= \frac{B(\omega_p, \omega_g)}{\alpha^{\chi - \omega_p} \beta^{\omega_p} (g - p)} = \gamma(\alpha, \beta, p, g, \chi). \end{aligned} \tag{12}$$

Therefore, according to Definition 4, the synchronized ST has the LUB of $T_{\text{least}} = \gamma(\alpha, \beta, p, g, \chi)$.

Next, the time-synchronized feature will be shown by using the ratio persistence condition. This part will be proved by contradiction.

Assume there exist two state elements x_i and x_j that converge separately. Without loss of generality, denote their ST as T_i, T_j, respectively, with $i \ne j$ and $T_j > T_i$. It indicates that x_i reaches the equilibrium earlier than x_j. Since x_i and x_j are RP, according to Lemma 2,

$$\lim_{t \uparrow T_i} x_i(t) = c_{ij} \lim_{t \uparrow T_i} x_j(t),$$

where c_{ij} is a non-zero constant parameter. T_i is the ST of x_i and $\lim_{t \uparrow T_i} x_i(t) = 0$, which yields

$$c_{ij} \lim_{t \uparrow T_i} x_j(t) = 0.$$

The continuous of the system (1) leads to $x_j(T_i) = 0$. It contradicts that x_j does not reach zero at T_i. Therefore the ST of each state element is synchronized.

Remark 3. In comparison to the conventional fixed-time stability [24,25], the theorem emphasizes the time synchronization property of the convergence, where ratio persistence is required as the mathematical foundation. Compared with the conventional ST estimation, especially with the method in [16] that inspires the proposed estimation, the theorem reformulates it as a Lyapunov condition that fits the vector case. Moreover, the LUB presented in the theorem is specifically calculated for the FTSC and cannot be directly used in classical sign-function-based fixed-time controllers.

3.2. Disturbance observer for fixed-time-synchronized control

Inspired by [26–28], a disturbance observer is designed, which converges to the true value in a fixed time.

$$\begin{aligned} \dot{\boldsymbol{z}}_0 &= -k_1 \mathrm{sig}_{\mathrm{c}}^{\frac{1}{2}}(\tilde{\boldsymbol{z}}_0) - k_2 \mathrm{sig}_{\mathrm{c}}^{\lambda}(\tilde{\boldsymbol{z}}_0) + \boldsymbol{f}_0 + \boldsymbol{G}_0 \boldsymbol{u} + \boldsymbol{z}_1, \\ \dot{\boldsymbol{z}}_1 &= -k_3 \mathrm{sign}_{\mathrm{c}}(\tilde{\boldsymbol{z}}_0), \end{aligned} \tag{13}$$

where $\lambda > 1$ is a constant parameter, $k_i > 0$ with $i = 1, 2, 3$, $\boldsymbol{z}_0$ and $\boldsymbol{z}_1$ are the estimated vector of system state $\boldsymbol{x}_2$ and the unknown external disturbance Δ, respectively. The observation error of the second-order state is defined as $\tilde{\boldsymbol{z}}_0 = \boldsymbol{z}_0 - \boldsymbol{x}_2$ and the disturbance observation error is constructed as $\tilde{\boldsymbol{z}}_1 = \boldsymbol{z}_1 - \Delta$.

Theorem 2. *Considering the system (7) and the disturbance observer (13), under Assumption 1, $\tilde{\boldsymbol{z}}_0$ and $\tilde{\boldsymbol{z}}_1$ converge to zero within the following enhanced time-bound*

$$T_{ob} \le \gamma_{ob} + \frac{\sigma + M\gamma_{ob}}{(1 - Mh/k_1)\, m} + \frac{\sigma}{m}, \tag{14}$$

where h, M, m and γ_{ob} have the forms

$$\begin{aligned} h &= \frac{1}{k_1} + \left(\frac{2e}{mk_1}\right)^{\frac{1}{3}}, & M &= k_3 + \delta, \\ \gamma_{ob} &= \gamma\left(2k_1, 2k_2, \frac{3}{4}, \frac{1+\lambda}{2}, 1\right), & m &= k_3 - \delta, \end{aligned} \tag{15}$$

and the following inequalities hold:

$$k_3 > \delta, k_1 > Mh. \tag{16}$$

Proof. From (13), the error dynamics is further derived

$$\begin{aligned} \dot{\tilde{\boldsymbol{z}}}_0 &= -k_1 \mathrm{sig}_{\mathrm{c}}^{\frac{1}{2}}(\tilde{\boldsymbol{z}}_0) - k_2 \mathrm{sig}_{\mathrm{c}}^{\lambda}(\tilde{\boldsymbol{z}}_0) + \tilde{\boldsymbol{z}}_1, \\ \dot{\tilde{\boldsymbol{z}}}_1 &= -k_3 \mathrm{sign}_{\mathrm{c}}(\tilde{\boldsymbol{z}}_0) - \dot{\Delta}. \end{aligned} \tag{17}$$

The bound in (14) is calculated by considering the following two situations:

Case 1: For every element i, $i = 1, \ldots, n$, $\mathrm{sign}_{\mathrm{c}}(\tilde{z}_{1,i}(0)) = 0$ or $\mathrm{sign}_{\mathrm{c}}(\tilde{z}_{1,i}(0)) = -\mathrm{sign}_{\mathrm{c}}(\tilde{z}_{0,i}(0))$.

Construct the Lyapunov function $V_{ob} = \tilde{\boldsymbol{z}}_0^{\mathrm{T}} \tilde{\boldsymbol{z}}_0$ with the following derivative

$$\dot{V}_{ob} = -2k_1 \tilde{\boldsymbol{z}}_0^{\mathrm{T}} \mathrm{sig}_c^{\frac{1}{2}}(\tilde{\boldsymbol{z}}_0) - 2k_2 \tilde{\boldsymbol{z}}_0^{\mathrm{T}} \mathrm{sig}_c^{\lambda}(\tilde{\boldsymbol{z}}_0) + 2\tilde{\boldsymbol{z}}_0^{\mathrm{T}} \tilde{\boldsymbol{z}}_1.$$

In this case, each element $\mathrm{sign_c}(\tilde{z}_{1,i})$ has either the opposite sign with respect to $\mathrm{sign_c}(\tilde{z}_{0,i})$ or the zero value, which leads to $\tilde{\boldsymbol{z}}_0^{\mathrm{T}}\tilde{\boldsymbol{z}}_1 \le 0$. Define $V_{ob,i} = \tilde{z}_{0,i}^2$ for $i = 1, \dots, i$, where $\tilde{z}_{0,i}$ is the ith element of $\tilde{\boldsymbol{z}}_0$. Therefore we have

$$\begin{aligned}\dot{V}_{ob,i} &\le -2k_1\tilde{z}_{0,i}\mathrm{sig}_c^{\frac{1}{2}}\left(\tilde{z}_{0,i}\right) - 2k_2\tilde{z}_{0,i}\mathrm{sig}_c^{\lambda}\left(\tilde{z}_{0,i}\right)\\ &= -2k_1V_{ob,i}^{\frac{3}{4}} - 2k_2V_{ob,i}^{\frac{1+\lambda}{2}}.\end{aligned}$$

The above equation has the same structure as (10) with $\chi = 1, \alpha = 2k_1, \beta = 2k_2, p = 3/4$ and $g = (1+\lambda/2)$. Following (11)–(12), $\tilde{z}_{0,i}$ is fixed-time stable for $i = 1, 2, \dots, n$, and the ST has the following LUB,

$$T_{ob1} \le \gamma_{ob} = \gamma\left(2k_1, 2k_2, \frac{3}{4}, \frac{1+\lambda}{2}, 1\right). \tag{18}$$

In the case of $\left\|\tilde{\boldsymbol{z}}_0(0)\right\| \to +\infty$, we have $T_{ob1} = \gamma_{ob}$.

When $t = T_{ob1}$, $\tilde{z}_{1,i}(T_{ob1})$ is bounded as

$$\left|\tilde{z}_{1,i}(T_{ob1})\right| \le \sigma + MT_{ob1}.$$

Considering $t > T_{ob1}$, $\tilde{z}_{1,i}(T_{ob1})$ starts at $(0, \sigma + MT_{ob1})$ for $i = 1, \dots, i$. Following Theorem 4.5 in [27] and the derivations in [26], with the condition of $Mh/k_1 < 1$, the ST of $\tilde{z}_{1,i}(T_{ob1})$ is bounded as

$$T_{ob2} \le \frac{\sigma + MT_{ob1}}{\left(1 - Mh/k_1\right)m}. \tag{19}$$

Therefore the ST of the disturbance observer (13) is bounded by

$$T_{ob}^{(1)} \le T_{ob1} + T_{ob2} \le \gamma_{ob} + \frac{\sigma + M\gamma_{ob}}{\left(1 - Mh/k_1\right)m}.$$

Case 2: There exist an element i, $i = 1, \dots, n$, such that $\mathrm{sign_c}(\tilde{z}_{1,i}(0)) = \mathrm{sign_c}(\tilde{z}_{0,i}(0))$.

We consider the case that there exists a dimension that $\mathrm{sign_c}(\tilde{\boldsymbol{z}}_1(0))$ and $\mathrm{sign_c}(\tilde{\boldsymbol{z}}_0(0))$ have the same sign, and $\tilde{z}_{0,i}$ cannot reach zero before $\mathrm{sign_c}(\tilde{z}_{1,i}) = -\mathrm{sign_c}(\tilde{z}_{0,i})$. Thus $\tilde{z}_{1,i}$ converges before $\tilde{z}_{0,i}$. From (17), we can derive that $\tilde{z}_{1,i}$ arrives at the origin within

$$T_{ob0} \le \frac{\sigma}{m}.$$

Next, when $t \ge T_{ob0}$, we have $\mathrm{sign_n}(\tilde{z}_1(T_{ob0})) = 0$ or for $i = 1, \dots, n$, $\mathrm{sign_c}(\tilde{z}_{1,i}(T_{ob0})) = -\mathrm{sign_c}(\tilde{z}_{0,i}(T_{ob0}))$, which has been discussed in Case 1. Repeat the derivation in Case 1, T_{ob1} in (18) becomes

$$T_{ob1}^* = T_{ob0} + T_{ob1}.$$

Then, the original T_{ob2} in (19) becomes

$$T_{ob2}^* \le \frac{M\gamma_{ob}}{\left(1 - Mh/k_1\right)m}.$$

The overall ST in this case takes the form

$$\begin{aligned}T_{ob}^{(2)} &\le T_{ob1}^* + T_{ob2}^*\\ &= \left(1 + \frac{1}{\left(1/M - h/k_1\right)m}\right)\gamma_{ob} + \frac{\sigma}{m}.\end{aligned}$$

Case 3: There exist an element i, $i = 1, \dots, n$, such that $\mathrm{sign_c}(\tilde{z}_{1,i}(0)) \ne 0$ and $\tilde{z}_{0,i}(0) = 0$.

In this situation, we have

$$\mathrm{sig}_c^{\frac{1}{2}}\left(\tilde{z}_{0,i}\right) = \mathrm{sig}_c^{\lambda}\left(\tilde{z}_{0,i}\right) = 0, \tag{20}$$

which leads to

$$\dot{\tilde{z}}_{0,i} = \dot{z}_{0,i} - \dot{x}_{2,i} = f_{0,i} + \left[g_0u\right]_i + z_{1,i} - \dot{x}_{2,i}, \tag{21}$$

where $\left[g_0u\right]_i$ indicates the ith dimension of g_0u. Substitute the formulation of $\dot{x}_2$ into the above equation yields

$$\dot{\tilde{z}}_{0,i} = z_{1,i} - \Delta_i = \tilde{z}_{1,i}. \tag{22}$$

Recall that in this case $\mathrm{sign_c}(\tilde{z}_{1,i}) \ne 0$, which leads to $\dot{\tilde{z}}_{0,i} \ne 0$. Thus, $\tilde{z}_{0,i}(0) = 0$ is a short enough transient process and it becomes Case 1 or Case 2 within $T_o b^{(3)} \to 0$.

From $T_{ob}^{(1)}$, $T_{ob}^{(2)}$ and $T_{ob}^{(3)}$, the enhanced ST is

$$T_{ob} \le \gamma_{ob} + \frac{\sigma}{m} + \frac{\sigma + M\gamma_{ob}}{\left(1 - Mh/k_1\right)m}. \tag{23}$$

Remark 4. In comparison to the super-twisting-based ST estimation in [26–28], Theorem 2 presents an enhanced ST estimation that consists of several stabilizing stages. Moreover, in some of the estimation methods, e.g., in [29], the observed disturbance/uncertainty $\tilde{\boldsymbol{z}}_1$ is required to be zero initially, whereas $\tilde{\boldsymbol{z}}_1(0)$ is allowed to be any finite value in Theorem 2.

3.3. Fixed-time-synchronized controller design and convergence analysis

On the basis of the proposed observer (13), we can design the controller for system (7).

Consider the sliding-mode manifold,

$$\boldsymbol{s} = \boldsymbol{x}_2 + \alpha_1\mathrm{sig_n^{p_1}}\left(\boldsymbol{x}_1\right) + \beta_1\mathrm{sig_n^{g_1}}\left(\boldsymbol{x}_1\right), \tag{24}$$

where α_1, β_1, p_1 and g_1 are positive constants, $0 < p_1 = p_1^*/p_2^* < 1$ and $g_1 = g_1^*/g_2^* > 1$. p_1^*, p_2^*, g_1^* and g_2^* are positive odd integers. In accordance with (24), the following result are presented.

Lemma 3. *For the sliding variable (24), when the sliding manifold stables with $\boldsymbol{s} = 0$, the system state $\boldsymbol{x}_1$ in system (7) is RP and the system is FTSS. Moreover, its synchronized settling time has the following LUB,*

$$T_{\mathrm{least}} = \gamma\left(\alpha_1, \beta_1, p_1, g_1, 1\right).$$

Proof. After the sliding manifold surface converges to $s = 0$,

$$\boldsymbol{x}_2 = -\alpha_1\mathrm{sig_n^{p_1}}\left(\boldsymbol{x}_1\right) - \beta_1\mathrm{sig_n^{g_1}}\left(\boldsymbol{x}_1\right). \tag{25}$$

Recall that $\dot{\boldsymbol{x}}_1 = \boldsymbol{x}_2$,

$$\begin{aligned}\frac{\dot{\boldsymbol{x}}_1}{\|\dot{\boldsymbol{x}}_1\|} &= \frac{-\left(\alpha_1\|\boldsymbol{x}_1\|^{p_1} + \beta_1\|\boldsymbol{x}_1\|^{g_1}\right)\mathrm{sign_n}\left(\boldsymbol{x}_1\right)}{\left\|-\left(\alpha_1\|\boldsymbol{x}_1\|^{p_1} + \beta_1\|\boldsymbol{x}_1\|^{g_1}\right)\mathrm{sign_n}\left(\boldsymbol{x}_1\right)\right\|}\\ &= -\frac{\mathrm{sign_n}\left(\boldsymbol{x}_1\right)}{\|\mathrm{sign_n}\left(\boldsymbol{x}_1\right)\|} = -\frac{\boldsymbol{x}_1}{\|\boldsymbol{x}_1\|}.\end{aligned} \tag{26}$$

From Definition 2, $\boldsymbol{x}_1$ is RP.

Consider a Lyapunov candidate $V = \boldsymbol{x}_1^{\mathrm{T}}\boldsymbol{x}_1$ with the following derivative

$$\dot{V} = 2\boldsymbol{x}_1^{\mathrm{T}}\boldsymbol{x}_2 = -2\alpha_1\boldsymbol{x}_1^{\mathrm{T}}\mathrm{sig_n^{p_1}}(\boldsymbol{x}_1) - 2\beta_1\boldsymbol{x}_1^{\mathrm{T}}\mathrm{sig_n^{g_1}}(\boldsymbol{x}_1).$$

From Definition 3, the above equation becomes

$$\begin{aligned}\dot{V} &= -2\alpha_1\boldsymbol{x}_1^{\mathrm{T}}\boldsymbol{x}_1\|\boldsymbol{x}_1\|^{p_1-1} - 2\beta_1\boldsymbol{x}_1^{\mathrm{T}}\boldsymbol{x}_1\|\boldsymbol{x}_1\|^{g_1-1}\\ &= -2\alpha_1\|\boldsymbol{x}_1\|^{p_1+1} - 2\beta_1\|\boldsymbol{x}_1\|^{g_1+1},\end{aligned} \tag{27}$$

where $\|\boldsymbol{x}_1\| = \sqrt{V}$, therefore

$$\dot{V} = -2\alpha_1V^{\frac{1+p_1}{2}} - 2\beta_1V^{\frac{1+g_1}{2}}.$$

From Theorem 1, FTSS is achieved and the synchronized ST has the following LUB,

$$T_{\mathrm{least}} = \gamma\left(2\alpha_1, 2\beta_1, \frac{1+p_1}{2}, \frac{1+g_1}{2}, 1\right).$$

The proof finishes here.

The possible singularity problem may be caused by the FTSC designed directly on (24). It happens at $x_1, x_2 \to 0$. The controller should be designed to be singularity-free. For such a purpose, the switching technique is adopted and the sliding mode manifold is modified to switch according to different situations. The modified controller is formulated as

$$\boldsymbol{u} = -\boldsymbol{G}_0^{-1}\left(\alpha_2\mathrm{sig_n^{p_2}}(\boldsymbol{s}) + \beta_2\mathrm{sig_n^{g_2}}(\boldsymbol{s}) + \dot{\boldsymbol{s}}_s + \boldsymbol{f}_0 + \boldsymbol{z}_1\right), \tag{28}$$

where $p_2 = p_3^*/p_4^* \in (0,1)$ and $g_2 = g_3^*/g_4^* \in (1, +\infty)$, p_3^*, p_4^*, g_3^* and g_4^* are positive odd integers.

$$\boldsymbol{s}_s = \begin{cases}\alpha_1\mathrm{sig_n^{p_1}}\left(\boldsymbol{x}_1\right) + \beta_1\mathrm{sig_n^{g_1}}\left(\boldsymbol{x}_1\right),\\ \quad \text{if } \boldsymbol{s}^* = 0 \text{ or } \boldsymbol{s}^* \ne 0,\ \|\boldsymbol{x}_1\| > \varepsilon,\\ l_1\boldsymbol{x}_1 + l_2\mathrm{sig_n^4}(\boldsymbol{x}_1),\\ \quad \text{if } \boldsymbol{s}^* \ne 0,\ \|\boldsymbol{x}_1\| \le \varepsilon,\end{cases} \tag{29}$$

$$\dot{s}_s = \begin{cases} \rho_1 x_1 x_1^{\mathrm{T}} x_2 + \rho_2 x_2, \\ \quad \text{if } s^* = 0 \text{ or } s^* \neq 0,\ \|x_1\| > \varepsilon, \\ l_1 x_2 + 3 l_2 \|x_1\| x_1 x_1^{\mathrm{T}} x_2 + l_2 \|x_1\|^3 x_2, \\ \quad \text{if } s^* \neq 0,\ \|x_1\| \leq \varepsilon, \end{cases} \tag{30}$$

In (28), the switching sliding variable is constructed by using a switching law s_s,

$$s = x_2 + s_s. \tag{31}$$

where x_2 is the system state. The derivative of s_s is presented in (29) and (30), where ε is a positive constant small enough and s^* is the trigger variable for the switching law,

$$s^* = x_2 + \alpha_1 \mathrm{sig}_{\mathrm{n}}^{p_1}(x_1) + \beta_1 \mathrm{sig}_{\mathrm{n}}^{g_1}(x_1), \tag{32}$$

variables ρ_1 and ρ_2 are formulated as

$$\rho_1 = \alpha_1 (p_1 - 1) \|x_1\|^{p_1 - 3} + \beta_1 (g_1 - 1) \|x_1\|^{g_1 - 3}, \tag{33}$$

$$\rho_2 = \alpha_1 \|x_1\|^{p_1 - 1} + \beta_1 \|x_1\|^{g_1 - 1}, \tag{34}$$

and constants l_1 and l_2 take the following forms

$$l_1 = \alpha_1 \left(\frac{4}{3} - \frac{p_1}{3}\right) \|\varepsilon\|^{p_1 - 1} + \beta_1 \left(\frac{4}{3} - \frac{g_1}{3}\right) \|\varepsilon\|^{g_1 - 1}, \tag{35}$$

$$l_2 = \alpha_1 \left(\frac{p_1}{3} - \frac{1}{3}\right) \|\varepsilon\|^{p_1 - 4} + \beta_1 \left(\frac{g_1}{3} - \frac{1}{3}\right) \|\varepsilon\|^{g_1 - 4}, \tag{36}$$

where p_1 and g_1 are re-written as

$$\frac{1}{2} < p_1 = p_1^*/p_2^* < 1, 1 < g_1 = g_1^*/g_2^* < 4,$$

where p_1^*, p_2^*, g_1^* and g_2^* are positive odd integers. The rationale of the parameter ranges can be found later in the proof of Theorem 4.

It can be verified that l_1 and l_2 are the critical designs to guarantee that s_s (29) and $\dot{s}_s$ (30) are continuous. Thus we have the following theorem.

Theorem 3. *Consider system (7) under Assumption 1, by designing the disturbance observer as in (13) and the control law as in (28), the sliding-mode variable s in (31) keeps a persistent ratio when $\tilde{z}_1 = 0$, x is RP when $s = 0$ and the system is FTSS with the settling time bounded by*

$$T_c \leq T_{ob} + \gamma_{c1} + \gamma_{c2}, \tag{37}$$

where T_{ob} is present in (14), γ_{c1} and γ_{c2} are gamma functions defined as

$$\gamma_{c1} = \gamma\left(2\alpha_1, 2\beta_1, \frac{1 + p_1}{2}, \frac{1 + g_1}{2}, 1\right),$$

$$\gamma_{c2} = \gamma\left(2\alpha_2, 2\beta_2, \frac{1 + p_2}{2}, \frac{1 + g_2}{2}, 1\right).$$

Proof. The proof will be conducted at $t \geq T_{ob}$, where T_{ob} is the enhanced ST for the disturbance observer. When $t \geq T_{ob}$, $\tilde{z}_1 = 0$ according to Theorem 2, leading to $z_1 = \Delta$.

A Lyapunov candidate $V_{c2} = s^{\mathrm{T}} s$ is considered in this stage, where

$$\dot{s} = \dot{x}_2 + \dot{s}_s = f_0(x_1, x_2) + G_0(x_1, x_2) u + \Delta + \dot{s}_s.$$

Substituting (28) into the above equation,

$$\begin{aligned} \dot{s} &= -\alpha_2 \mathrm{sig}_{\mathrm{n}}^{p_2}(s) - \beta_2 \mathrm{sig}_{\mathrm{n}}^{g_2}(s) - z_1 + \Delta \\ &= -\alpha_2 \mathrm{sig}_{\mathrm{n}}^{p_2}(s) - \beta_2 \mathrm{sig}_{\mathrm{n}}^{g_2}(s), \end{aligned}$$

therefore we have

$$\frac{\dot{s}}{\|\dot{s}\|} = -\frac{\alpha_2 \mathrm{sig}_{\mathrm{n}}^{p_2}(s) + \beta_2 \mathrm{sig}_{\mathrm{n}}^{g_2}(s)}{\|\alpha_2 \mathrm{sig}_{\mathrm{n}}^{p_2}(s) + \beta_2 \mathrm{sig}_{\mathrm{n}}^{g_2}(s)\|}.$$

Since $\mathrm{sig}_{\mathrm{n}}^{\alpha}(s) = \|s\|^{\alpha} \mathrm{sign}_{\mathrm{n}}(s)$,

$$\begin{aligned} \frac{\dot{s}}{\|\dot{s}\|} &= -\frac{(\alpha_2 \|s\|^{p_2} + \beta_2 \|s\|^{g_2}) \mathrm{sign}_{\mathrm{n}}(s)}{\|(\alpha_2 \|s\|^{p_2} + \beta_2 \|s\|^{g_2}) \mathrm{sign}_{\mathrm{n}}(s)\|} \\ &= -\frac{\mathrm{sign}_{\mathrm{n}}(s)}{\|\mathrm{sign}_{\mathrm{n}}(s)\|} = -\frac{s}{\|s\|}, \end{aligned}$$

indicating that s is RP when $t \geq T_{ob}$. Moreover, $\dot{V}_{c2}$ becomes

$$\begin{aligned} \dot{V}_{c2} &= 2 s^{\mathrm{T}} \left(-\alpha_2 \mathrm{sig}_{\mathrm{n}}^{p_2}(s) - \beta_2 \mathrm{sig}_{\mathrm{n}}^{g_2}(s)\right) \\ &= -2\alpha_2 V_{c2}^{\frac{1 + p_2}{2}} - 2\beta_2 V_{c2}^{\frac{1 + g_2}{2}}, \end{aligned}$$

therefore s is FTSS and the synchronized ST has the following LUB,

$$T_{c2} \leq \gamma_{c2} = \gamma\left(2\alpha_2, 2\beta_2, \frac{1 + p_2}{2}, \frac{1 + g_2}{2}, 1\right). \tag{38}$$

The above process can be understood as a stage which the observer has converged to the true value and the sliding manifold s is approaching its equilibrium. When $t \geq T_{ob} + T_{c2}$, the sliding manifold s keeps zero. Since $s = x_2 + s_s$, we can obtain

$$x_2 = -s_s = \begin{cases} -\alpha_1 \mathrm{sig}_{\mathrm{n}}^{p_1}(x_1) - \beta_1 \mathrm{sig}_{\mathrm{n}}^{g_1}(x_1), \\ \quad \text{if } s^* = 0 \text{ or } s^* \neq 0,\ \|x_1\| > \varepsilon, \\ -l_1 x_1 - l_2 \mathrm{sig}_{\mathrm{n}}^{4}(x_1), \\ \quad \text{if } s^* \neq 0,\ \|x_1\| \leq \varepsilon. \end{cases}$$

Similar to the analysis of s, the above equation indicates that the state x_1 is RP.

By using Lemma 3 and the ratio persistence property, the FTSS of the state x_1 can be guaranteed, and the enhanced synchronized ST for x_1 to converge along $s = 0$ can be written as

$$T_{c1} \leq \gamma_{c1} = \gamma\left(2\alpha_1, 2\beta_1, \frac{1 + p_1}{2}, \frac{1 + g_1}{2}, 1\right). \tag{39}$$

Thus, for the disturbed system (24), the overall enhanced synchronized setting time of x_1 takes the form

$$T_c \leq T_{ob} + T_{c1} + T_{c2}, \tag{40}$$

thus the proof ends.

Remark 5. Note that $T_{ob} + T_{c1} + T_{c2}$ calculated in (37) is not the LUB of T_c. It has a different form with the T_{least} in Definition 4. More accurately speaking, it is regarded as the *enhanced* estimation for T_c. The calculated T_c in (37) consists of three parts, namely T_{ob}, T_{c1} and T_{c2}, which are the LUBs for different stages of the stabilizing process. In the estimations of T_{c1} and T_{c2}, the derivatives of the Lyapunov functions appear as equations instead of relaxed inequations due to the specific property of the time-synchronized stability. Therefore, (37) is less overestimated than its counterparts in conventional fixed-time control results. The comparison between the proposed estimation and the conventional estimation will be further conducted and analyzed in the simulation part.

The singularity-free property of the controller (28) is demonstrated below.

Theorem 4. *The possible singularity problem of system (7) is avoided under the controller (28) and the switching sliding manifold (31).*

Proof. The analysis is conducted in three cases:

(1) $\|x_1\| > \varepsilon$, where no singularity exists obviously.

(2) $\|x_1\| \leq \varepsilon$, $s^* \neq 0$, where the sliding-mode manifold (31) becomes generalized according to the switching law (29) and no singularity occurs apparently.

(3) $\|x_1\| \leq \varepsilon$, $s^* = 0$, from (28) and (29), it yields

$$u = -G_0^{-1} \left(\alpha_2 \mathrm{sig}_{\mathrm{n}}^{p_2}(s) + \beta_2 \mathrm{sig}_{\mathrm{n}}^{g_2}(s) + f_0 + J(x_1)\right), \tag{41}$$

where $J(x_1)$ is defined by

$$\begin{aligned} J(x_1) =& \alpha_1 \rho_1 x_1 x_1^{\mathrm{T}} \mathrm{sig}_{\mathrm{n}}^{p_1}(x_1) + \beta_1 \rho_1 x_1 x_1^{\mathrm{T}} \mathrm{sig}_{\mathrm{n}}^{g_1}(x_1) \\ &+ \alpha_1 \rho_2 \mathrm{sig}_{\mathrm{n}}^{p_1}(x_1) + \beta_1 \rho_2 \mathrm{sig}_{\mathrm{n}}^{g_1}(x_1). \end{aligned} \tag{42}$$

Substituting ρ_1 and ρ_2 (introduced in (33)–(34)) into (42) and noticing $x_1 x_1^{\mathrm{T}} \mathrm{sig}_{\mathrm{n}}^{p_1}(x_1) = \mathrm{sig}_{\mathrm{n}}^{p_1 + 2}(x_1)$, we have

$$\begin{aligned} J(x_1) =& \alpha_1^2 p_1 \mathrm{sig}_{\mathrm{n}}^{2p_1 - 1}(x_1) + \beta_1^2 g_1 \mathrm{sig}_{\mathrm{n}}^{2g_1 - 1}(x_1) \end{aligned}$$

$$+\alpha_1\beta_1\left(p_1+g_1\right)\mathrm{sig}_{\mathrm{n}}^{p_1+g_1-1}\left(\boldsymbol{x}_1\right). \tag{43}$$

Since $\frac{1}{2} < p_1 < 1$ and $g_1 > 1$, the singularity is avoided.

Remark 6. For (29), the sliding manifold $\boldsymbol{s}_s = l_1\boldsymbol{x}_1 + l_2\mathrm{sig}_{\mathrm{n}}^4(\boldsymbol{x}_1)$ only works at $s^* \neq 0$ and $\|\boldsymbol{x}_1\| \leq \varepsilon$. When a small enough value is selected for ε, the trajectory of the system state $\boldsymbol{x}_1$ will be governed by $\boldsymbol{s}_s = \alpha_1\mathrm{sig}_{\mathrm{n}}^{p_1}\left(\boldsymbol{x}_1\right) + \beta_1\mathrm{sig}_{\mathrm{n}}^{g_1}\left(\boldsymbol{x}_1\right)$ instead of $\boldsymbol{s}_s = l_1\boldsymbol{x}_1 + l_2\mathrm{sig}_{\mathrm{n}}^4(\boldsymbol{x}_1)$. Although $\boldsymbol{s}_s = l_1\boldsymbol{x}_1 + l_2\mathrm{sig}_{\mathrm{n}}^4(\boldsymbol{x}_1)$ does not work much with a small enough ε, the convergence property of this situation can still be analyzed.

Remark 7. Many useful methods have been presented for the singularity problem, among which the switching sliding-mode manifold is proved to be quite effective. The sliding manifold (31) is inspired by [30], where a switching law is adopted for the avoidance of the singularity problem. The switching manifold has been used in spacecraft attitude tracking [31,32], however, it is not applicable to $\mathrm{sig}_{\mathrm{n}}(\cdot)^{\alpha}$ due to its special design for the classical sign function. The proposed switching manifold is designed based on $\mathrm{sign}_{\mathrm{n}}(\boldsymbol{x}_1)$ and each element in vector $\boldsymbol{x}_1$ is considered in (29). To summarize, this approach extends the scalar formulation of the super-twisting sliding mode surface to a generalized multi-dimensional case by using the norm-normalized sign function, thus the controller design and convergence analysis procedures differ from the existing results significantly. The proposed switching law (29) is newly designed with a different structure, its contribution lies in both avoiding the singularity point and achieving FTSC.

4. Comparative simulations

In the simulations, the proposed controller (28) is examined to verify its FTSC property and the enhanced estimation. Firstly, the control law (28) is modified to be non-synchronized for a comprehensive comparison.

Lemma 4. *Considering the system (7), by using the disturbance observer (13) and the following control law*

$$\bar{\boldsymbol{u}} = -\boldsymbol{G}_0^{-1}\left(\alpha_2\mathrm{sig}_{\mathrm{c}}^{p_2}(\bar{\boldsymbol{s}}) + \beta_2\mathrm{sig}_{\mathrm{c}}^{g_2}(\bar{\boldsymbol{s}}) + \dot{\bar{\boldsymbol{s}}}_s + \boldsymbol{f}_0 + \boldsymbol{z}_1\right), \tag{44}$$

the system converges in a fixed time.

In (44), $\bar{\boldsymbol{s}} = \boldsymbol{x}_2 + \bar{\boldsymbol{s}}_s$ is the sliding manifold, $\bar{\boldsymbol{s}}^* = \boldsymbol{x}_2 + \alpha_1\mathrm{sig}_{\mathrm{c}}^{p_1}\left(\boldsymbol{x}_1\right) + \beta_1\mathrm{sig}_{\mathrm{c}}^{g_1}\left(\boldsymbol{x}_1\right)$ is the trigger sliding-mode variable, and (45)–(46) presents the switching law.

$$\bar{\boldsymbol{s}}_{s,i} = \begin{cases} \alpha_1\mathrm{sig}_{\mathrm{c}}^{p_1}\left(x_{1,i}\right) + \beta_1\mathrm{sig}_{\mathrm{c}}^{g_1}\left(x_{1,i}\right), \\ \quad \text{if } \bar{\boldsymbol{s}}^* = 0, \text{ or } \bar{\boldsymbol{s}}^* \neq 0, \ |x_{1,i}| > \varepsilon, \\ l_3x_{1,i} + l_4\mathrm{sig}_{\mathrm{c}}^2\left(x_{1,i}\right), \\ \quad \text{if } \bar{\boldsymbol{s}}^* \neq 0, \ |x_{1,i}| \leq \varepsilon, \end{cases} \tag{45}$$

$$\dot{\bar{\boldsymbol{s}}}_{s,i} = \begin{cases} \alpha_1p_1|x_{1,i}|^{p_1-1}x_{2,i} + \beta_1g_1|x_{1,i}|^{g_1-1}x_{2,i}, \\ \quad \text{if } \bar{\boldsymbol{s}}^* = 0, \text{ or } \bar{\boldsymbol{s}}^* \neq 0, \ |x_{1,i}| > \varepsilon, \\ l_3x_{2,i} + l_4\left|x_{1,i}\right|x_{2,i}, \\ \quad \text{if } \bar{\boldsymbol{s}}^* \neq 0, \ |x_{1,i}| \leq \varepsilon, \end{cases} \tag{46}$$

In (45)–(46), the subscript i represents the ith element in the corresponding vector, l_3 and l_4 are constant parameters designed to keep the continuity of $\bar{\boldsymbol{s}}_s$ and $\dot{\bar{\boldsymbol{s}}}_s$. The formulation of l_3 and l_4 are as follows

$$l_3 = (2-p_1)\alpha_1\varepsilon^{p_1-1} + (2-g_1)\beta_1\varepsilon^{g_1-1}, \tag{47}$$

$$l_4 = (p_1-1)\alpha_1\varepsilon^{p_1-2} + (g_1-1)\beta_1\varepsilon^{g_1-2}. \tag{48}$$

Proof. The proof can be obtained as the derivation process for Theorem 3.

Remark 8. Comparing controller (44) and controller (28), it can be figured out clearly that the system state in different dimensions is controlled separately. Due to this reason, the synchronized convergence cannot be achieved by using controller (44). The controller (44) has the same form as (28) except for the sign functions and the time-synchronization property. Comparative experiments are conducted between them to highlight the merits generated by this difference.

Remark 9. The modified switching law $\bar{\boldsymbol{s}}_s$ in (44) is a conventional design for fixed-time control and basically has the same structure as the ones in [30–32], where detailed analysis and proof can be found. In Lemma 4, $\bar{\boldsymbol{s}}_{s,i}$ is constructed by the classical sign function $\mathrm{sig}_{\mathrm{c}}(x_{1,i})$ for fixed-time stability. It is calculated according to every element $x_{1,i}$ of the system state separately. In contrast, the proposed switching law in our approach (29) is designed based on $\mathrm{sig}_{\mathrm{n}}(\boldsymbol{x}_1)$ for FTSC. It is calculated as a vector according to $\boldsymbol{x}_1$. Due to the difference between $\mathrm{sig}_{\mathrm{c}}(\boldsymbol{x}_1)$ and $\mathrm{sig}_{\mathrm{n}}(\boldsymbol{x}_1)$, the formulation of sliding manifolds $\bar{\boldsymbol{s}}_s$ and $\boldsymbol{s}_s$, the calculation of constant parameters l_i, and the construction of triggering variable $\bar{s}^*$ differ significantly. In summary, the forms of these designs are the fundamental difference between the proposed work and the existing ones, which lead to different performances.

Remark 10. The time-synchronization phenomenon comes from the norm-normalized sign function $\mathrm{sig}_{\mathrm{n}}(\boldsymbol{x}_1)$. Many existing fixed-time-synchronized control methods can be extended with such stability. For example, fixed-time-synchronized convergence of multi-agent systems can be referred to at our previous work [33]. However, time-synchronized stability requires that every element of the system couples with each other, thus it will change the communication topology if used in distributed control, e.g., [34,35].

In Table 2, the simulation parameters are presented. To produce a fair comparison, the same parameters are shared by controller (28) and controller (44).

Table 2
Simulation parameters.

Parameters	Values	Parameters	Values
$\boldsymbol{f}_0$	$5\boldsymbol{x}$	$\boldsymbol{G}_0$	$2\boldsymbol{I}_3$, $\boldsymbol{I}$ is the identity matrix
k_1	10	k_2	50
k_3	20	λ	11/9
δ	0.657	θ	0.0001
α_1	1	α_2	5
β_1	0.2	β_2	0.2
p_1	7/13	p_2	7/13
g_1	15/9	g_2	15/9
Δ	$[2, 3\sin(0.02\pi t), 4\sin(0.05\pi t + \pi/2)]^{\mathrm{T}}$		

Fig. 1 illustrates the state $\boldsymbol{x}$ by using the proposed controller (28) and the compared controller (44), respectively. Using the proposed control law (28), each element of $\boldsymbol{x}$ arrives at their equilibrium simultaneously under disturbances, while using (44), the elements of $\boldsymbol{x}$ reach the equilibrium at separate time instants. This phenomenon can be figured out more clearly in Fig. 2, where the absolute state values are illustrated. In the plots, the state elements converge at $t = 6.3$ s time-synchronously by using the proposed control law (28), whereas they reach the equilibrium at 2.1 s, 4.5 s, and 6.3 s by using the control law (44). In Fig. 2, we zoom on the plots around the arrival time instant at the level of $\times 10^{-4}$, where the time-synchronization property of the state elements can be figured out clearly.

The input signals of the two controllers are illustrated in Fig. 3. The amount of energy consumed by the proposed controller (28) is calculated as $E = \sum_{i=1}^{n}\int_0^T u_i^2(\tau)\mathrm{d}\tau$, and the energy consumed by the fixed-time controller (44) is computed by $\bar{E} = \sum_{i=1}^{n}\int_0^T \bar{u}_i^2(\tau)\mathrm{d}\tau$. The control energy are compared and illustrated in the first plot of Fig. 4, which indicates that less energy is needed by the proposed controller than the compared controller.

The second figure of Fig. 4 plots the ratio of different pairs of state elements, namely $x_{1,k}/x_{1,j}, k \neq j$. In the plots, the RP property under the controller (28) is verified, where the ratio of each pair becomes time-invariant after a short time period T_{ob}. Subfigures for the initial

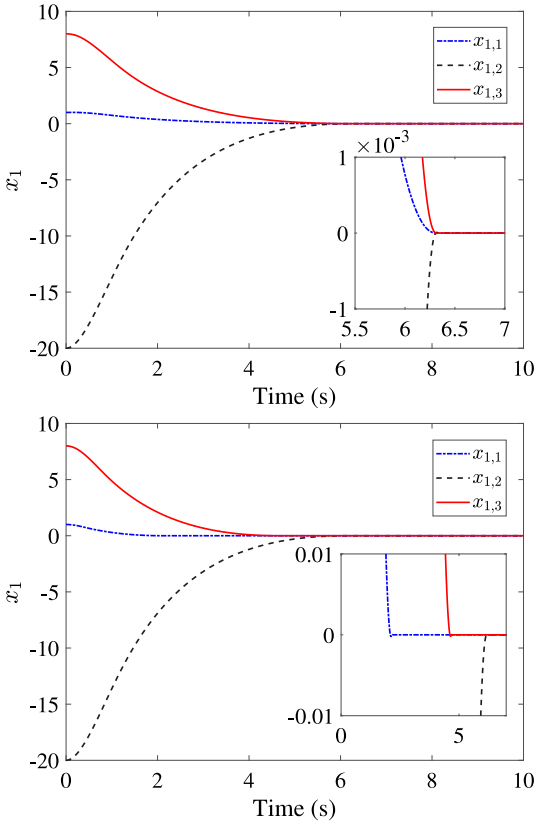

Fig. 1. System state $\boldsymbol{x}$ by using the proposed controller (up) and the compared law (44) (down), respectively.

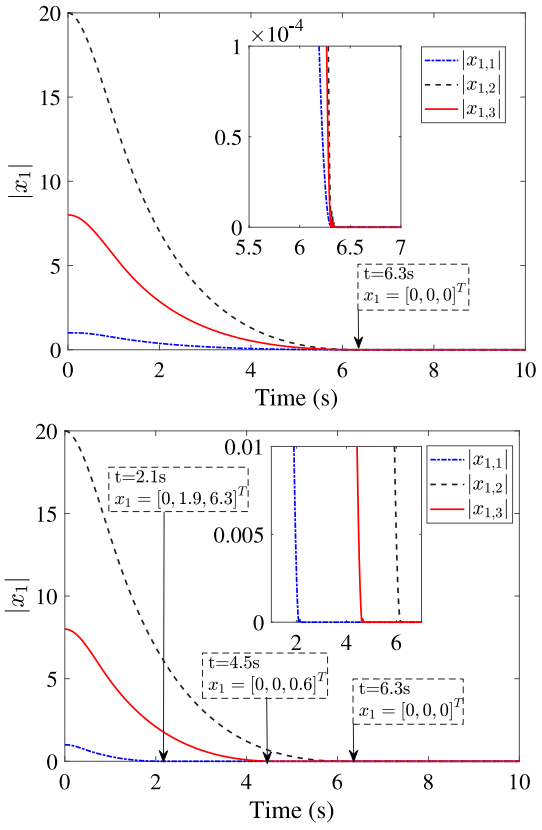

Fig. 2. Norms of $x_{1,i}$ by using the proposed control law (up) and the compared control law (down), respectively.

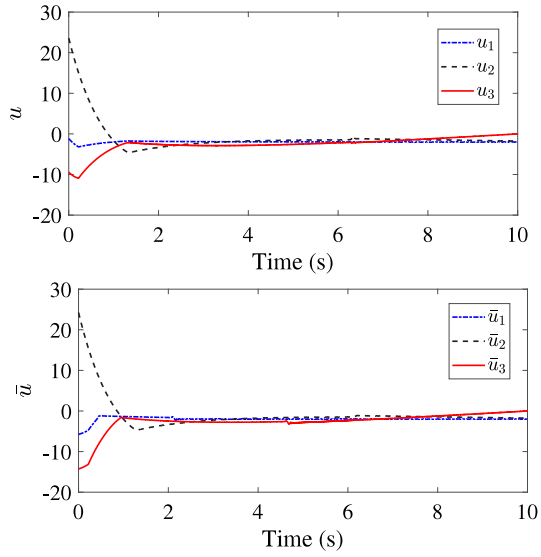

Fig. 3. Control inputs under the proposed controller (28) (up) and the compared controller (44) (down).

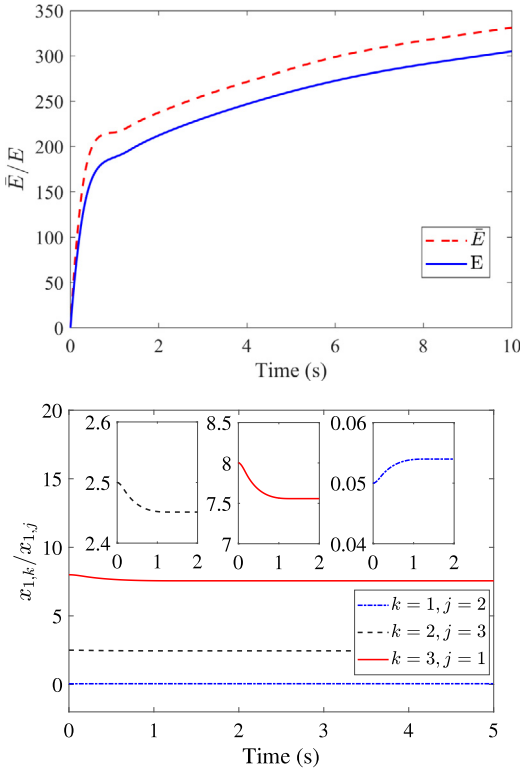

Fig. 4. Up: Energy consumed by the proposed method (E) and the compared method ($\bar{E}$). Down: Every pair of state elements keeps the persistent ratio.

time period are illustrated to show the detailed convergence process of the state ratio. Moreover, the FTSC can also be checked in this figure.

Fig. 5 presents the 3-D state trajectories by using controller (28) and controller (44). The trajectory by the proposed control law is plotted

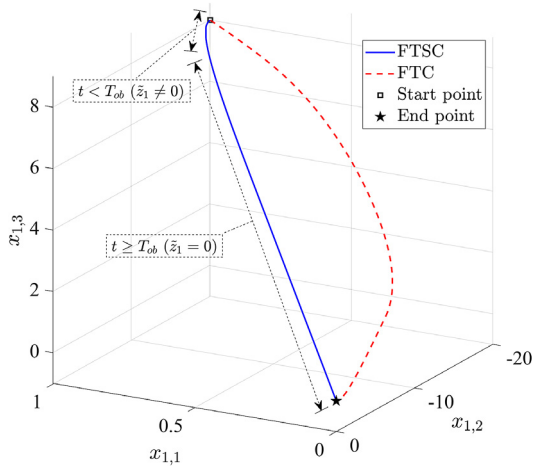

Fig. 5. Trajectory plots of system states generated by using the proposed and compared controllers.

by the blue line, and can be divided into two parts. The first part is generated by $t < T_{ob}$, where the disturbance estimation achieved by the disturbance observer (13) is not the accurate value, namely $\tilde{z}_1 \neq 0$. The second part is the $t \geq T_{ob}$ part, where accurate disturbance estimation can be used as known information. In this case, a smoother and shorter trajectory can be generated by the proposed method due to the influence of the fixed-time-synchronized property. When precise disturbance estimation is achieved with $\tilde{z}_1 = 0$ and $t \geq T_{ob}$, according to Theorem 3, the output state trajectory is RP. As in the figure, an RP state trajectory shows up as a straight line, which can be taken as optimal from the perspective of the trajectory length. In contrast, the red state trajectory, which is generated by the fixed-time law (44), appears much longer and more unpredictable than the blue trajectory.

In what follows, the enhanced ST estimation is verified in the simulations, whose performance is compared with the famous work in (40). The proposed estimation is calculated with the parameters in Table 2,

$$\begin{aligned} T_c \leq & T_{ob} + T_{c1} + T_{c2} \\ = & \gamma\left(2k_1, 2k_2, \frac{3}{4}, \frac{1+\lambda}{2}, 1\right) + \frac{\sigma + M\gamma_{ob}}{\left(1 - Mh/k_1\right)m} \\ & + \frac{\sigma}{m} + \gamma\left(2\alpha_1, 2\beta_1, \frac{1+p_1}{2}, \frac{1+g_1}{2}, 1\right) \\ & + \gamma\left(2\alpha_2, 2\beta_2, \frac{1+p_2}{2}, \frac{1+g_2}{2}, 1\right) \\ = & 9.3019 \text{ s}. \end{aligned} \tag{49}$$

With the same parameters, a typical work on the ST estimation [5] generates the following result,

$$\begin{aligned} \bar{T}_c \leq & \bar{T}_{ob} + \bar{T}_{c1} + \bar{T}_{c2} \\ = & \frac{1}{k_1(1-3/4)} + \frac{2}{k_2(\lambda - 1)} + \frac{\sigma + M\gamma_{ob}}{\left(1 - Mh/k_1\right)m} \\ & + \frac{\sigma}{m} + \frac{1}{\alpha_1(1-p_1)} + \frac{1}{\beta_1(g_1 - 1)} \\ & + \frac{1}{\alpha_2(1-p_2)} + \frac{1}{\beta_2(g_2 - 1)} \\ = & 19.2464 \text{ s}. \end{aligned} \tag{50}$$

The proposed estimation (49) and the classical estimation (50) can be used for both controllers (28) and controller (44). Apparently, the proposed enhanced estimation generates a better result, which is less overestimated than the classical estimation. Fig. 6 shows clearly that by using our method, the proposed estimation T_c is substantially closer to the real value of the ST compared to the estimation $\bar{T}_c$ from [5]. The reasons are in two aspects. Firstly, the enhanced estimation consists of several LUBs for different stabilizing stages. Secondly, the LUBs are calculated by un-relaxed Lyapunov derivative equations that are more accurate than commonly used relaxed inequations. A detailed comparison between T_c and $\bar{T}_c$ is further studied by using an example. Let $\alpha_1 = \alpha_2 = \varpi$ and $\beta_1 = \beta_2 = 1/\varpi$ with a positive variable ϖ, and other parameters remain the same. The ratio between $\bar{T}_c(\varpi)$ and $T_c(\varpi)$ is illustrated in Fig. 7, where $\forall \varpi > 0, \bar{T}_c/T_c > 1$. In the special case of $\varpi \to \infty$ or $\varpi \to 0$, the ratio goes to infinity. The validity of the enhanced ST estimation is thus demonstrated.

Remark 11. The proposed estimation of the LUB for the ST has shown good performance, however, the advantage lies in the specific property of the time-synchronized convergence. When it is used for conventional fixed-time control, the estimation may not be as good as in the paper.

5. Conclusion

This paper has considered the fixed-time-synchronized control problem for disturbed affine systems and the estimation for the least upper bound of the settling time. A relevant Lyapunov theorem has been proposed for the fixed-time-synchronized control, and corresponding controllers have been designed for multivariable disturbed systems that are singularity-free. An enhanced estimation for the least upper bound of the synchronized settling time is presented which is constructed by several least upper bounds, and the calculated value is less overestimated than the existing results. An emerging deeper perception is brought for fixed-time stability by this paper. In the future, the time-synchronized convergence will be developed for more complex requirements such as predefined-time control and prescribed performance control.

CRediT authorship contribution statement

Wanyue Jiang: Writing – original draft, Funding acquisition. **Shuzhi Sam Ge:** Conceptualization. **Ruihang Ji:** Validation. **Dongyu Li:** Methodology.

Declaration of competing interest

Shuzhi Sam Ge, Ruihang Ji, and Dongyu Li are associate editors for *Journal of Automation and Intelligence* and was not involved in the editorial review or the decision to publish this article. All authors declare that there are no competing interests.

Acknowledgments

This work was supported by the National Natural Science Foundation of China under Grant No. 62303256 and Shandong Higher Education Youth Innovation and Science Fund Support Program No. 2023KJ362.

Data availability

No data was used for the research described in the article.

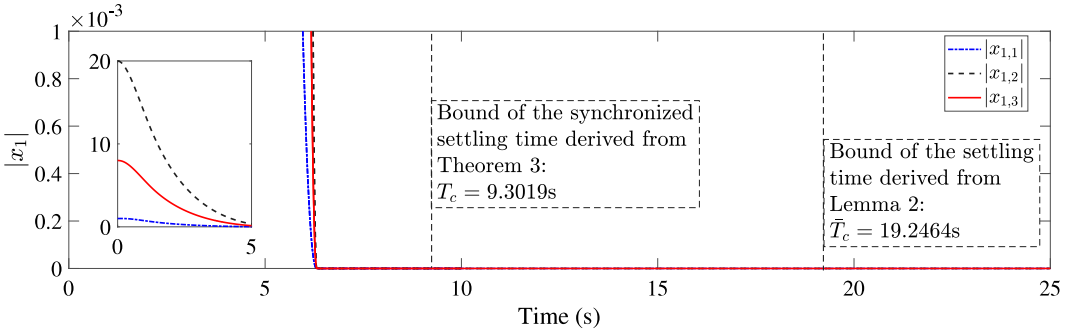

Fig. 6. Absolute state value x by using the proposed controller (28), with the proposed enhanced estimation T_c and the estimation $\bar{T}_c$ derived in [5].

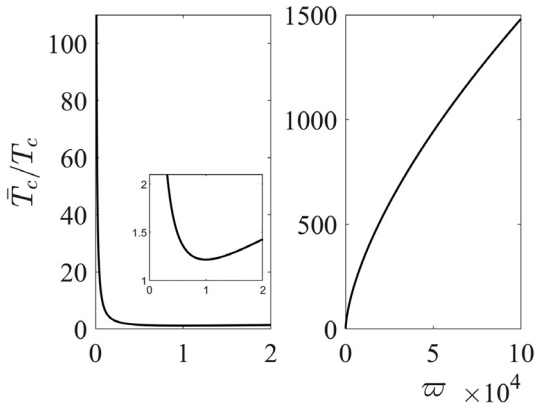

Fig. 7. A comparison between T_c in (49) and $\bar{T}_c$ in (50).

References

[1] S.P. Bhat, D.S. Bernstein, Finite-time stability of continuous autonomous systems, SIAM J. Control Optim. 38 (3) (2000) 751–766.

[2] P. Liu, S. Tong, A finite-time fuzzy adaptive output-feedback fault-tolerant control for underactuated wheeled mobile robots systems, J. Autom. Intell. (2024).

[3] H. Ren, H. Ma, H. Li, Z. Wang, Adaptive fixed-time control of nonlinear MASs with actuator faults, IEEE/ CAA J. Autom. Sin. 10 (5) (2023) 1252–1262.

[4] T.N. Truong, A.T. Vo, H.-J. Kang, A model-free terminal sliding mode control for robots: Achieving fixed-time prescribed performance and convergence, ISA Trans. 144 (2024) 330–341.

[5] A. Polyakov, Nonlinear feedback design for fixed-time stabilization of linear control systems, IEEE Trans. Autom. Control 57 (8) (2012) 2106–2110.

[6] Y.-c. Zhang, M.-c. Ma, X.-Y. Yang, S.-m. Song, Disturbance-observer-based fixed-time control for 6-DOF spacecraft rendezvous and docking operations under full-state constraints, Acta Astronaut. 205 (2023) 225–238.

[7] X. Li, C. Wen, J. Wang, Lyapunov-based fixed-time stabilization control of quantum systems, J. Autom. Intell. 1 (1) (2022) 100005.

[8] D. Zhang, J. Hu, J. Cheng, Z.-G. Wu, H. Yan, A novel disturbance observer based fixed-time sliding mode control for robotic manipulators with global fast convergence, IEEE/ CAA J. Autom. Sin. 11 (3) (2024) 661–672.

[9] C. Hua, W. Tian, Q. Li, Switching event-triggered fixed-time control for uncertain high-order nonlinear systems, IEEE Trans. Autom. Control (2024).

[10] Y. Song, H. Ye, F.L. Lewis, Prescribed-time control and its latest developments, IEEE Trans. Syst. Man, Cybern.: Syst. 53 (7) (2023) 4102–4116.

[11] S. Chen, H. Jiang, Z. Yu, F. Zhao, Distributed optimization of single-integrator systems with prescribed-time convergence, IEEE Syst. J. (2022).

[12] G. Di Mauro, M. Lawn, R. Bevilacqua, Survey on guidance navigation and control requirements for spacecraft formation-flying missions, J. Guid. Control Dyn. 41 (3) (2018) 581–602.

[13] D. Li, S.S. Ge, T.H. Lee, Simultaneous-arrival-to-origin convergence: Sliding-mode control through the norm-normalized sign function, IEEE Trans. Autom. Control (2021).

[14] W. Jiang, S.S. Ge, Q. Hu, D. Li, Sliding-mode control for perturbed MIMO systems with time-synchronized convergence, IEEE Trans. Cybern. (2023).

[15] M. Basin, Finite- and fixed-time convergent algorithms: Design and convergence time estimation, Annu. Rev. Control. 48 (2019) 209–221.

[16] R. Aldana-López, D. Gómez-Gutiérrez, E. Jiménez-Rodríguez, J.D. Sánchez-Torres, M. Defoort, Enhancing the settling time estimation of a class of fixed-time stable systems, Internat. J. Robust Nonlinear Control 29 (12) (2019) 4135–4148.

[17] H. Zhou, Y. Song, V. Tzoumas, Safe non-stochastic control of control-affine systems: An online convex optimization approach, IEEE Robot. Autom. Lett. (2023).

[18] W. Chen, Q. Wei, A new optimal adaptive backstepping control approach for nonlinear systems under deception attacks via reinforcement learning, J. Autom. Intell. 3 (1) (2024) 34–39.

[19] I. Nagesh, C. Edwards, A multivariable super-twisting sliding mode approach, Automatica 50 (3) (2014) 984–988.

[20] S.S. Butt, H. Aschemann, Multi-variable integral sliding mode control of a two degrees of freedom helicopter, IFAC- Pap. 48 (1) (2015) 802–807.

[21] L. Zhang, C. Wei, R. Wu, N. Cui, Fixed-time extended state observer based non-singular fast terminal sliding mode control for a VTVL reusable launch vehicle, Aerosp. Sci. Technol. 82 (2018) 70–79.

[22] H. Bateman, Higher Transcendental Functions [Volumes I-III], 1, McGraw-Hill Book Company, 1953.

[23] M. Basin, P. Yu, Y. Shtessel, Finite- and fixed-time differentiators utilising HOSM techniques, IET Control Theory Appl. 11 (8) (2017) 1144–1152.

[24] S.M. Esmaeilzadeh, M. Golestani, S. Mobayen, Chattering-free fault-tolerant attitude control with fast fixed-time convergence for flexible spacecraft, Int. J. Control. Autom. Syst. 19 (2) (2021) 767–776.

[25] C. Hu, H. Jiang, Special functions-based fixed-time estimation and stabilization for dynamic systems, IEEE Trans. Syst. Man, Cybern.: Syst. (2021) 1–12.

[26] V. Utkin, On convergence time and disturbance rejection of super-twisting control, IEEE Trans. Autom. Control 58 (8) (2013).

[27] Y. Shtessel, C. Edwards, L. Fridman, A. Levant, Sliding Mode Control and Observation, Springer, 2014.

[28] M. Basin, C.B. Panathula, Y. Shtessel, Multivariable continuous fixed-time second-order sliding mode control: Design and convergence time estimation, IET Control Theory Appl. 11 (8) (2017) 1104–1111.

[29] X. Wang, J. Guo, S. Tang, S. Qi, Fixed-time disturbance observer based fixed-time back-stepping control for an air-breathing hypersonic vehicle, ISA Trans. 88 (2019) 233–245.

[30] L. Wang, T. Chai, L. Zhai, Neural-network-based terminal sliding-mode control of robotic manipulators including actuator dynamics, IEEE Trans. Ind. Electron. 56 (9) (2009) 3296–3304.

[31] K. Lu, Y. Xia, Adaptive attitude tracking control for rigid spacecraft with finite-time convergence, Automatica 49 (12) (2013) 3591–3599.

[32] B. Jiang, Z. Chen, Q. Hu, J. Qi, Fixed-time attitude control for rigid spacecraft with actuator saturation and faults, IEEE Trans. Control Syst. Technol. 24 (5) (2014) 4375–4380.

[33] D. Li, S.S. Ge, T.H. Lee, Fixed-time-synchronized consensus control of multiagent systems, IEEE Trans. Control. Netw. Syst. 8 (1) (2021) 89–98.

[34] X. Hu, L. Wang, C.-K. Zhang, Y. He, Fixed-time synchronization of fuzzy complex dynamical networks with reaction-diffusion terms via intermittent pinning control, Trans. Fuz Sys. 32 (4) (2024) 2307–2317.

[35] G. Zhang, J. Cao, Aperiodically semi-intermittent-based fixed-time stabilization and synchronization of delayed discontinuous inertial neural networks, Sci. China Inf. Sci. 68 (1) (2025) 112202.

Wanyue Jiang received the M.Sc. and Ph.D. degrees in control theory and engineering from the Nanjing University of Aeronautics and Astronautics, Nanjing, China, in 2015 and 2019, respectively. She is currently an Associate Professor with the Automation School, Qingdao University, Qingdao, China. Her main research interests include control theory, artificial intelligence, and robotics.

Shuzhi Sam Ge received the B.Sc. degree in control engineering from the Beijing University of Aeronautics and Astronautics, Beijing, China, in 1986, and the Ph.D. degree in robotics from Imperial College London, London, U.K., in 1993. He is currently the Director of the Social Robotics Laboratory of Smart Systems Institute, National University of Singapore, Singapore, where he is also a Professor with the Department of Electrical and Computer Engineering. He is also the Honorary Director of the Institute for Future, Qingdao University, Qingdao China. He has (co)authored seven books and over 300 international journal articles and conference papers. His current research interests include robotics, intelligent systems, artificial intelligence, and smart materials. Prof. Ge is also the Editor-in-Chief of the International Journal of Social Robotics (Springer). He has been serving as an Associate Editor for a number of flagship journals, including the IEEE TRANSACTIONS ON AUTOMATIC CONTROL, the IEEE TRANSACTIONS ON CONTROL SYSTEMS TECHNOLOGY, the IEEE TRANSACTIONS ON SYSTEMS, MAN, AND CYBERNETICS: SYSTEMS, Automatica, and the CAAI Transactions on Intelligence Technology. He also serves as a Book Editor for the Taylor and Francis Automation and Control Engineering Series.

Ruihang Ji received the B.S. and Ph.D. degree from Control Science and Engineering, Harbin Institute of Technology, China, in 2016 and 2021. He was a joint Ph.D. student supported by China Scholarship Council with the Department of Electrical and Computer Engineering at National University of Singapore, where he is currently a Research Fellow with the Institute for Functional Intelligent Materials. His current research interests include nonlinear control, secure networked systems, and human–robot interaction.

Dongyu Li received the B.S. and Ph.D. degrees in control science and engineering from the Harbin Institute of Technology, China, in 2016 and 2020, respectively. From 2017 to 2019, he was a joint Ph.D. student with the Department of Electrical and Computer Engineering, National University of Singapore, Singapore. where he was a Research Fellow with the Department of Biomedical Engineering, from 2019 to 2021. He is currently an Associate Professor with the School of Cyber Science and Technology, Beihang University, Beijing, China. His research interests include networked system cooperation, adaptive systems, and spacecraft engineering.